Wide-Band Channel Measurements at 60GHz in Indoor Environments

Jeetinder Purwaha, Arthur Mank, Dušan Matic, Klaus Witrisal and Ramjee Prasad
Center for Wireless Personal Communications (CEWPC), IRCTR
Delft University of Technology, Mekelweg 4, 2628 CD Delft, The Netherlands
Tel.: +31/15/278-1782; Fax: +31/15/278-1774; E-mail: D.Matic@ITS.TUDelft.NL

Abstract: **Applying a recently proposed measuring principle** [1]**, the behavior of the wide-band indoor radio channel at 60 GHz was studied, using a measurement set-up consisting of a continuous wave signal generator and a spectrum analyzer was used.**

A new method described in [2], [3] **was used for the first time to extract the *rms* delay spread from non-coherent wide-band (WB) measurements.**

Three channel parameters were extracted from the measured power spectrum samples; the path loss exponent, Ricean K-factor and *rms* delay spread.

Two types of measurements were performed, continuous wave (CW) and WB. The investigated environments were a common room and a workshop.

I Introduction

Over the past few years, there has been an increasing emphasis upon extending the services available on fixed public telecommunication networks to mobile users. Multimedia and computer communications are also playing an increasing role in today's society, creating new challenges to those working in the development of telecommunication. At present, in addition to voice services, only low rate data services (about several kilobits per second) are available on a mobile basis. Future systems are looking to increase the data rate of the services on mobile communication systems.

First step, in order to implement such a system, is frequency allocation and selection. Next step is to understand the channel characteristics and, based on that, develop a radio channel model. The millimeter (mm) wave band from 20 – 60 GHz is seen by many researchers as a possible solution for wireless broadband communication systems [4] – [7]. This band has the potential to support broadband service access. Systems working particularly in the 60 GHz frequency band can have a small reuse distance, because of the oxygen absorption at the rate of 15 dB/km. Another advantage of 60 GHz is the fact that this frequency region is not being in use by any other communication medium, so every channel can be allocated a large bandwidth, e.g. 100 MHz may be used without any problem. Also, due to the small wavelength, the antenna size is very small, thus equipment will be compact.

This paper presents the results of non-coherent frequency domain (FD) measurements performed in the electrical engineering building at Delft University of Technology. A spectrum analyzer along with a continuous wave signal generator has been used to measure the channel's amplitude transfer function.

The wavelength at 60 GHz is just 5mm, thus great fluctuation of the received signal occur over small variations of the antenna separation, due to multipath interference. It is appropriate to quantify the channel behavior by measuring the parameters within a local area (has a diameter of 20λ), rather than channel parameters of one particular position. Two types of measurements were conducted, continuous wave (CW) and wide-band (WB). CW measurements were done by transmitting a 59.9 GHz sinusoid, while WB measurements were done by sweeping the CW signal over a bandwidth of 100 MHz around the center frequency of 59.9 GHz.

The measurement campaign was organized in two different indoor environments, the common room of the electrical engineering building of Delft University of Technology and a workshop located in the same building. The locations selected are based on the assumption of possible usage of mobile multimedia communication via a small terminal. A propagation database was set up from the measurements. These measurements were then used to obtain three important local area parameters; local area received power (p_o), Ricean K-factor and *rms* delay spread (τ_{rms}). Local area power (p_o) and the Ricean K-factor are obtained straightforwardly from the data set of a local area [9]. For the estimation of the *rms* delay spread (τ_{rms}) a completely new method is applied, using the level crossing rate (LCR) of the transfer function in the frequency domain [2], [3].

II Measurement Setup

The main goal of the measurements was to characterize the channel transfer function.

The measurement setup [1] used to perform the frequency domain measurements is given in Fig. 1. The two main components are a CW signal generator and a spectrum analyzer.

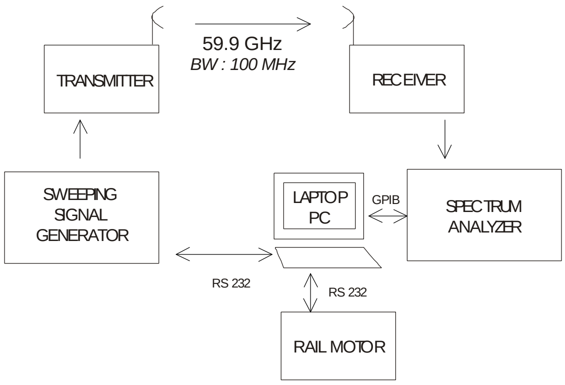

Figure 1: Measurement setup

Omnidirectional antennas (120°) were used at the transmitter and the receiver. The output of the signal generator is fed directly to the transmitter. Energy collected at the receiver is translated down to the IF. This signal is fed to the spectrum analyzer to determine the power frequency response of the channel. The data collected is stored in the computer for later analysis. To investigate the location variability of the channel, the receiver was placed on a computer-controlled cart running on rails. After measuring at a point, the cart is moved to next position.

The CW measurements were done at 59.9 GHz. During the WB measurements, a sinusoid was swept across 100 MHz bandwidth. The signal generator was controlled by the computer via RS-232 port. At each position, a spectrum of 1000 samples was obtained, with a step of 100 kHz resulting in a total bandwidth of 100 MHz.

The usual calibration, necessary with systems based on network analyzers, was not done. Complex, absolute values of the channel transfer function were not essential, since the method for extracting the channel parameters needs only relative alterations of the power over the bandwidth measured. However, the amplitude transfer-function of the system had to be considered and compensated for. The calibration in our case was done by measuring the transfer function of the measurement set-up (including the antennas) in the anechoic chamber. For our system, it was virtually flat and could be neglected.

III Description of Measurements

Measurements were performed in two indoor environments, a common room and a workshop. Since the channel has to be time-invariant for swept-frequency measurements, all measurements were performed at night or on weekends when there were few, if any, people in the vicinity of the measurement setup. In almost all measurements, a LOS (line of sight) component was present. The transmitter antenna was fixed, while the receiver was moved around to different positions. The area covered was on the order of a pico-cell (radius smaller than 50m) in both environments. Antenna height in all measurements was 1.60 m for both transmitter and receiver antenna.

Before the measurements could begin, a test was performed in order to determine the step between two successive WB measurements. The purpose was to get the distance after which there is no correlation between the spectrums. For the purpose of this test, 76 spectrum samples were collected with a step size of 0.4 mm.

It was concluded that the correlation between the spectra stops at approximately 5 mm distance (= 1λ on 60 GHz). It was decided to perform WB measurements at every 5 mm in each local area, of a diameter of 20λ (10 cm). CW measurements were performed with a step size of 1 mm (1/5λ) in each local area. A number of local areas were investigated in both sites.

First measurement site was the common room, a large room (56x10 m^2) filled with wooden tables and chairs. There are also 24 (1x1 m) concrete pillars in this room. Walls on three sides of the common room are made up of concrete and on one side of glass. A plot of the part of the room where measurements were conducted is given Fig. 2.

In total, WB measurements were done in 34 local areas and CW in 21 local areas in the common room. Along line L, both CW and WB measurements were conducted in order to compare the two measurement methods. The local areas were separated by 0.5 m, covering a distance range of 1.5 to 11.5 m. In each local area, 100 CW samples and 21 WB spectra were measured.

WB measurements were also conducted along three lines HW, HC and six other local areas in the common room. These local areas are given with a black dot in Fig. 2. Three of these local areas are on the side of the glass wall and three on the side of the canteen.

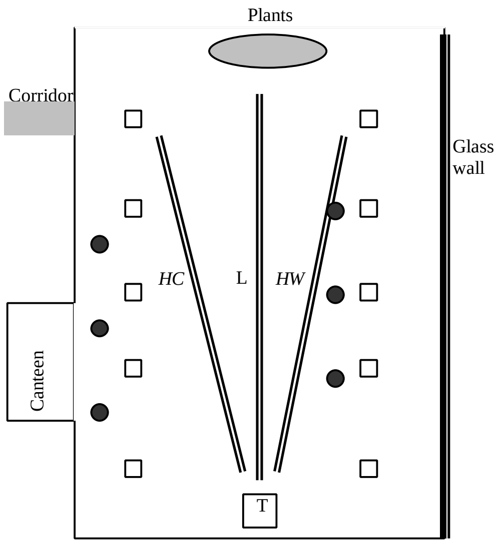

Figure 2: Measurement locations in the common room

The second measurement location was the work shop at the faculty building in order to see the propagation in a factory-like environment with heavy machines and less free space. In the workshop, only WB measurements were conducted.

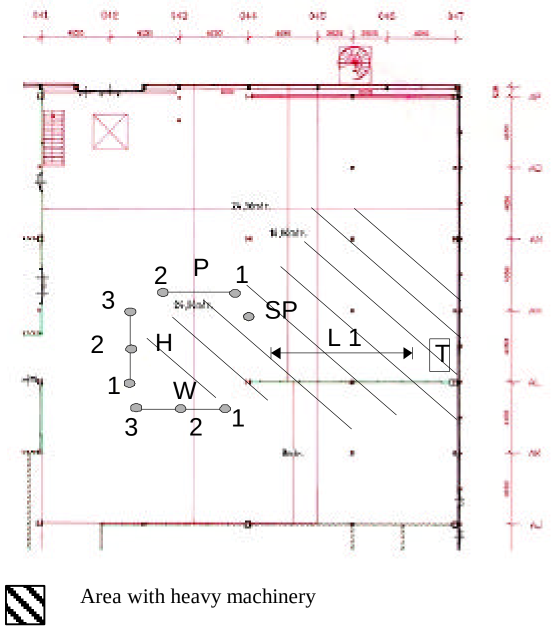

Figure 3: Measurement positions in the work shop placing transmitter in the area with heavy machinery

The workshop can be divided in two parts, the one with heavy machinery and the one with smaller machines. Measurements were performed placing the transmitter in both of them. Fig.3 illustrates the first position of the transmitter. There were 13 local areas investigated along line L1 between 1.5 m and 7.5 m antenna separation and 9 other local area as shown with a dot in Fig. 3

Second position of the transmitter antenna was in the part of the workshop with less concentration of machines. This position is shown in Fig. 4. Measurements were done along the two lines LT1 (4 local area spaced by 2.5 m) and LT2 (4 local area spaced by 3 m).

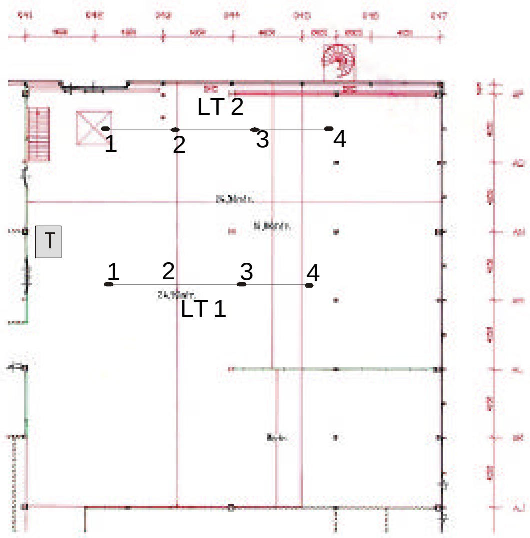

Figure 4: Measurements in work shop placing transmitter in the area with small machinery

IV Measurement Analysis

Due to the settings of the spectrum analyzer, a large amount of noise was contained in the WB measurements. A program emulating a low pass FIR (finite impulse response) filter was designed to filter the noise from the WB spectra. This filter had a cut-off frequency (f_c) of 0.05 times the Nyquist frequency and 40 coefficients. Hamming windowing was used in the filter design. There is one drawback in using this filter, because 40 sample points are lost from the original spectrum of 1000 samples.

Measurements were conducted with the purpose of characterizing the channel with three local area channel parameters, the local area received power (p_o), Ricean K-factor and the RMS delay spread (t_{rms}). All 21 spectra in each local area were joint together to extract these statistical parameters from one combined data set with a total equivalent bandwidth of approximately 2 GHz. This was done in order to get a sufficiently large spectrum sample for a statistically reliable analysis. For the CW measurements, 100 samples were collected in the same manner.

A. *Path loss exponent (a)*

Local area received power was extracted by averaging the 21·(1000 – 40) = 20160 samples of the combined data sets from WB measurements, and the 100 samples from CW measurements.

Received power (p_r) decreases with the distance (d) as

$$p_r = Cd^{-a} \tag{1}$$

where α is the exponent of the power-distance relationship and C is a constant set by transmitted power and measured system gain. α is also known as the path-loss exponent.

In this paper, the values of α were extracted only for the experiments when the transmitter and receiver antennae were aligned – line L in the common room and line L1 in the work shop.

B. *Ricean K-factor*

Dramatic changes in the signal amplitude and phase as a result of small variation in the spatial separation between the receiver and transmitter are referred to as small scale fading. The amplitude distribution of small scale fading is characterized by the Ricean probability distribution function (PDF) when a dominant LOS component is present. The Ricean K-factor is defined as the ratio between the LOS signal power and the variance of the multipath or power of the multipath component [8]. The Ricean PDF is given as [8]

$$f(r) = \begin{cases} \dfrac{r}{s^2} e^{-\frac{r^2+A^2}{2s^2}} \mathrm{I}_0\left(\dfrac{Ar}{s^2}\right), & r \ge 0 \\ 0, & r < 0 \end{cases} \tag{2}$$

where A denotes the peak amplitude of the dominant signal, s^2 is the power of the multipath components and $\mathrm{I}_0(\bullet)$ is the modified Bessel function of the first kind and zero-order. The Ricean K-factor is given as [8]

$$K = \frac{A^2}{2s^2} \tag{3}$$

The Ricean K-factor is extracted from the collected data set using the following expression [9]

$$\frac{E[r]}{\sqrt{E[r^2]}} = \sqrt{\frac{p}{4(K+1)}} \exp\left(-\frac{K}{2}\right) \times \left[(K+1)I_0\left(\frac{K}{2}\right) + KI_1\left(\frac{K}{2}\right)\right] \tag{4}$$

where E[r] is the average amplitude, $E[r^2]$ the average of the squared amplitude and $I_n(\bullet)$ is the modified Bessel function of the first kind and n-th order. Fig. 5 shows (4) graphically.

The K values that are generated by (4) are checked by plotting the cumulative distribution function (CDF) obtained using measured data and the theoretical CDF obtained using (3) and (2). The Kolmogorov-Smirnov test is used for the best fit test [9]. An example of a typical plot is shown in Fig. 6. The theoretical CDF that was obtained using (3) and (2), corresponds to K=12.20.

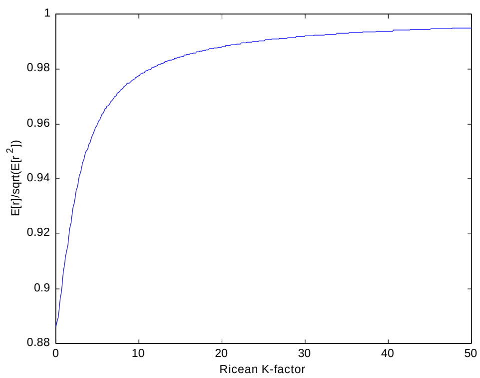

Figure 5: The relationship between the statistics of the received amplitude and the Ricean K-factor

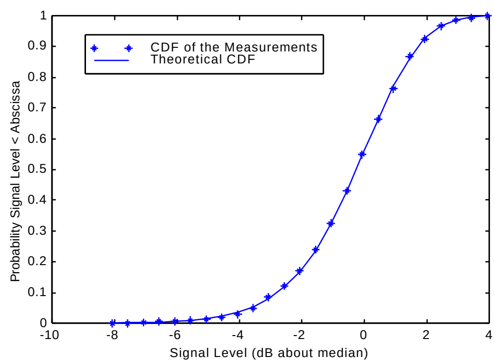

Figure 6: An example of a CDF plot of the measured data and the CDF corresponding to K=12.20

C. *RMS delay spread (t_{rms})*

Due to multipath propagation, the channel response is composed of rays with different paths. Each of these rays has its own amplitude gain, propagation delay and a phase shift. A radio channel can be modeled as a linear filter having an impulse response of the multiple paths. That can be expressed as

$$h(t) = \sum_{n=0}^{N-1} b_n \exp(-jq_n)\, d(t - t_n) \qquad (5)$$

where b_n is the amplitude, t_n is the delay and q_n is the phase shift associated with the n-th received ray.

Another characteristic of the channel in the time domain is the power delay profile, which is the power response of the channel. In the case of a δ-pulse transmitted, it is defined as

$$p(t) = |h(t)|^2 = \sum_{n=0}^{N-1} b_n^{\,2}\, d(t - t_n) \qquad (6)$$

The RMS delay spread (t_{rms}) is the square root of the second central moment of the power delay profile and is defined as

$$t_{rms} = \sqrt{\overline{t^2} - \overline{t}^2} \qquad (7)$$

where

$$\overline{t} = \frac{\sum_{n=0}^{N-1} p(t_n)\, t_n}{\sum_{n=0}^{N-1} p(t_n)} = \frac{\sum_{n=0}^{N-1} t_n b_n^{\,2}}{\sum_{n=0}^{N-1} b_n^{\,2}} \qquad (8)$$

and

$$\overline{t^2} = \frac{\sum_{n=0}^{N-1} t_n^{\,2} b_n^{\,2}}{\sum_{n=0}^{N-1} b_n^{\,2}} \qquad (9)$$

t_{rms} is a good measure of the multipath spread of the channel. It is used to estimate the potential of intersymbol interference.

A new method to extract *rms* delay spread from the level crossing rate (LCR) in the frequency domain was used to analyse the data. The LCR is defined as the rate at which the fading signal amplitude $R(f) = |H(f)|$ crosses a average signal level r in a positive going direction. The model used in this paper is based on a frequency-domain channel model (FD-model) characterized by the delay power spectrum (DPS) of the channel [3]. The shape of its dps is defined as shown in Fig. 7. It is characterized by four parameters

1. $p(0)$ [dB] the normalized power of the direct ray (LOS component)
2. Π [1/ns], the normalized power density of the constant-level part
3. τ_1 [ns], the duration of the constant level part
4. g [dB/ns], the slope of the exponentially decaying part

Based on this model, it can be shown mathematically that the LCR denoted by $N_R(r')$ can be expressed as

$$N_R(r') = t_{rms} \cdot f(K, u, r') \qquad (10)$$

where $r' = r/\sqrt{NRP}$ represents a normalized threshold variable and $u = t_1 \cdot g$ accounts for the shape of the DPS. Fig. 8 shows the factor $f(K,u,r')$ of $r' = 1$ and $u = 0$, i.e. at $r = \sqrt{NRP}$ and $t_1 = 0$. Using this figure, the measured LCR can be translated to t_{rms} [2].

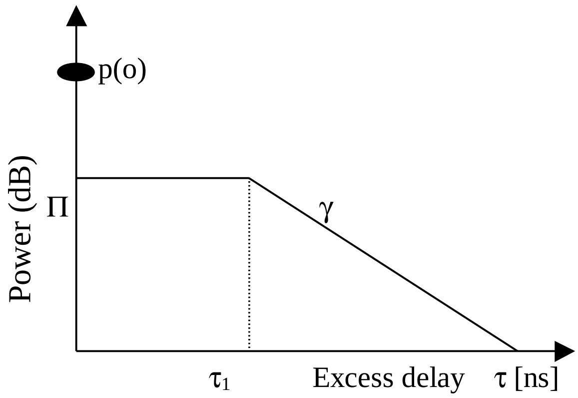

Figure 7: Model of the delay power spectrum

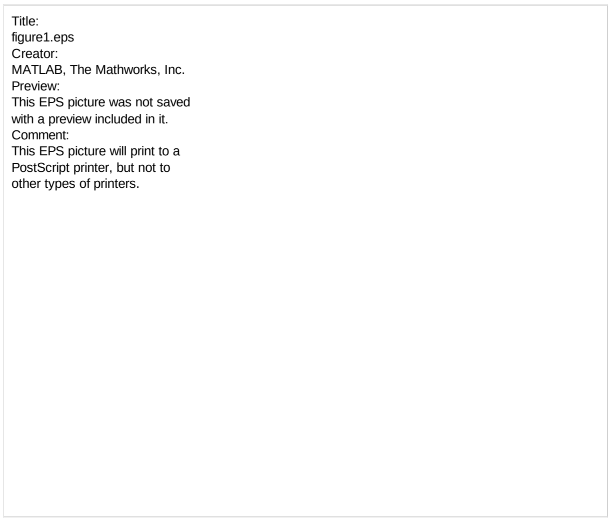

Figure 8: The proportionality factor relating the LCR to t_{rms}

Using the FD model and the frequency domain simulation scheme proposed in [3], one can re-generate channel transfer functions with the given K-factor, p_0 and t_{rms}, and simulate the frequency-selective fading.

V Results and Conclusions

The theoretical model for extracting t_{rms} from LCR, described in [2] and [3], using the spectrum analyzer data was used for the first time in practice. Results found in this paper show that this method works very well. One can get a good estimation of the time dispersion parameters from the frequency response measurements.

It was necessary to use filtering and to gather many spectrum samples in a local area, in order to get statistically reliable data.

Results obtained from the measurements in the common room are summarized in Table 1.

Along line L in the common room, both CW and WB measurements were performed. From the CW measurements, the path loss exponent and the K-factors were extracted. The results found from the two measurement methods were almost same. In Fig. 9, a plot is shown for the variation of the K-factor along line L with WB and CW measurements.

TABLE 1

Results for the channel parameters found in the common room

Parameter	Mean	Std. Dv.	Max.	Min.
a	0.9	-	-	-
K	11.25	13.31	60.1	0.60
t_{rms} **[ns]**	4.89	2.77	10	1.2

The maximum K-factor found in the common room was 60 and the minimum 0.60. Higher K-factors were found for the local area near the glass wall than near the canteen. Lower values of t_{rms} were found for the local area near the glass wall than for the local area near the canteen. Maximum t_{rms} was 10 ns.

Table 2 summarizes the results found in the workshop.

TABLE 2

Results of the channel parameters found in the work shop

Parameter	Mean	Std	Max.	Min.
a	1.13	-	-	-
K	8.19	6.19	27.40	1.70
t_{rms} **[ns]**	7.81	2.59	12	4

Less fading is also experienced in the measurements near the glass wall than in the measurements near the concrete wall.

If the transmitter and receiver antenna are aligned and a strong LOS component is present, as for measurement on L and L1, it is found that the K-factor decreases with distance, down to a certain level. In Fig. 9, this effect is shown for measured on line L in the common room. The *rms* delay spread (t_{rms}) is found to increase with the distance, also to a certain level.

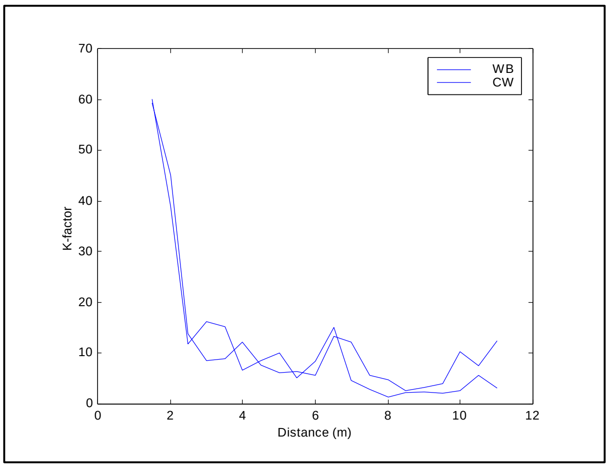

Figure 9: The change of the K-factor along line L in the common room

Acknowledgments

The authors would like to thank everybody in the IRCTR (International Research Center for Telecommunications-Transmission and Radar) group at Delft University of Technology for their help and cooperation. They would also like to express their gratitude to NEC and NWO (Dutch foundation for the development of science) for their support of this research. This work is a part of the MMC (Mobile Multimedia Communication) project. More information can be found on (http://mmc.et.tudelft.nl)

References

[1] D. Matic, H. Harada, R. Prasad: “Indoor and outdoor frequency domain measurements for mm-waves in the range of 60 GHz”, Proc. VTC’98, Ottawa, May 1998

[2] K.Witrisal, Y.H. Kim, and R.Prasad: "A novel rms delay spread estimation technique using non-coherent channel measurements", IEE Electronics Letter, Sept./Oct. 1998

[3] K.Witrisal, Y.H. Kim and Dr. R. Prasad: “Frequency domain simulation and analysis of the frequency selective Ricean fading radio channel”, PIMRC’98, Boston, Sep. 1998

[4] L.M. Correia, R. Prasad: “An Overview of Wireless Broadband Communications”, IEEE Communications Magazine, Jan. 1997, pp. 28-33

[5] S.W. Wales and D.C. Rickard: “Wideband propagation measurements of short range millimetric radio channels”, Electronics & Communication Engineering Journal, August 1993, pp. 249-254

[6] P.F.M. Smulders and A.G. Wagemans: “Wideband indoor radio propagation measurements at 58 GHz”, Electronics letters, Vol. 28, No. 13, June 1992, pp. 1270-1272

[7] M. Bensebti, J.P. Mc Geehan and M.A. Beach: “Indoor multipath radio propagation measurements and characterization at 60 GHz”, European Microwave Conf., Stuttgart Sep. 1991, pp. 1217-1222

[8] T.S. Rappaport: “Wireless Communications”, Prentice Hall, 1996

[9] Frank van der Wijk, A.Kegel and R. Prasad: "Assessment of a Pico-Cellular system using propagation measurements at 1.9 GHz for indoor wireless communications", IEEE Trans. on Veh. Tech., Vol. 44, No.1, Feb. 1995, pp 155-162.